The Cryosphere Discuss., 7, 5433–5460, 2013
www.the-cryosphere-discuss.net/7/5433/2013/
doi:10.5194/tcd-7-5433-2013

The Cryosphere Discussions
Open Access

ESA's Ice Sheets CCI: validation and inter-comparison of surface elevation changes derived from laser and radar altimetry over Jakobshavn Isbræ, Greenland – Round Robin results

J. F. Levinsen[1], K. Khvorostovsky[2], F. Ticconi[3,4], A. Shepherd[3], R. Forsberg[1], L. S. Sørensen[1], A. Muir[5], N. Pie[6], D. Felikson[6], T. Flament[7], R. Hurkmans[8], G. Moholdt[9], B. Gunter[10,11], R. C. Lindenbergh[10], and M. Kleinherenbrink[10]

[1]DTU Space, National Space Institute, Technical University of Denmark, Elektrovej, Building 327 + 328, 2800 Kongens Lyngby, Denmark
[2]Nansen Environmental and Remote Sensing Center, Thormøhlens gate 47, 5006 Bergen, Norway
[3]School of Earth and Environment, University of Leeds, Leeds LS2 9JT, UK
[4]EUMETSAT, Remote Sensing and Product Unit, Eumetsat Allee 1, 64295 Darmstadt, Germany
[5]University College London, Gower Street, London, WC1E 6BT, UK

[6]University of Texas, Center for Space Research, 3925 West Braker Lane, Suite 200, Austin, Texas 78759-5321, USA
[7]Laboratoire d'Études en Géophysique et Océanographie Spatiales (LEGOS), 14 avenue Edouard Belin, 31400 Toulouse, France
[8]Bristol Glaciology Centre, School of Geographical Sciences, University of Bristol, University Road, Bristol, BS8 1SS, UK
[9]Scripps Institution of Oceanography, 9500 Gilman Drive, La Jolla, 92093-0225, USA
[10]Department of Geoscience & Remote Sensing, Delft University of Technology, 2600 GA Delft, the Netherlands
[11]School of Aerospace Engineering, Georgia Institute of Technology, 270 Ferst Drive, Atlanta, GA 30332-0150, USA

Received: 17 October 2013 – Accepted: 4 November 2013 – Published: 15 November 2013

Correspondence to: J. F. Levinsen (jfl@space.dtu.dk)

Published by Copernicus Publications on behalf of the European Geosciences Union.

Abstract

In order to increase the understanding of the changing climate, the European Space Agency has launched the Climate Change Initiative (ESA CCI), a program which joins scientists and space agencies into 13 projects either affecting or affected by the concurrent changes. This work is part of the Ice Sheets CCI and four parameters are to be determined for the Greenland Ice Sheet (GrIS), each resulting in a dataset made available to the public: Surface Elevation Changes (SEC), surface velocities, grounding line locations, and calving front locations. All CCI projects have completed a so-called Round Robin exercise in which the scientific community was asked to provide their best estimate of the sought parameters as well as a feedback sheet describing their work. By inter-comparing and validating the results, obtained from research institutions world-wide, it is possible to develop the most optimal method for determining each parameter. This work describes the SEC Round Robin and the subsequent conclusions leading to the creation of a method for determining GrIS SEC values. The participants used either Envisat radar or ICESat laser altimetry over Jakobshavn Isbræ drainage basin, and the submissions led to inter-comparisons of radar vs. altimetry as well as cross-over vs. repeat-track analyses. Due to the high accuracy of the former and the high spatial resolution of the latter, a method, which combines the two techniques will provide the most accurate SEC estimates. The data supporting the final GrIS analysis stem from the radar altimeters on-board Envisat, ERS-1 and ERS-2. The accuracy of laser data exceeds that of radar altimetry; the Round Robin analysis has, however, proven the latter equally capable of dealing with surface topography thereby making such data applicable in SEC analyses extending all the way from the interior ice sheet to margin regions. This shows good potential for a future inclusion of ESA CryoSat-2 and Sentinel-3 radar data in the analysis, and thus for obtaining reliable SEC estimates throughout the entire GrIS.

1 Introduction

As the climate is changing, a global need has arisen for scientists and space agencies to combine their efforts into establishing long-term data records that will allow for observing the changes. This has led to the establishment of 13 Essential Climate Variables to be derived from satellite data acquired in ESA Earth Observation and Third Party missions as well by international partners. Each climate variable is an individual project, and the topics have been identified via the United Nations Framework Convention on Climate Change (UNFCCC). They must (ESA, 2011):

1. cover a representative set of variables for the ocean, Earth and atmosphere,
2. cover crucial elements of the carbon and water cycles,
3. address major, though poorly understood, climate radiative forcing and feedback mechanisms,
4. address the most rapidly changing elements of the climate system.

The 13 projects were launched in two stages, e.g. aerosol and cloud properties, glaciers and ozone in 2010 followed by sea-ice, soil moisture and ice sheets in 2011/2012. This work is part of the Ice Sheets CCI in which the focus area is the Greenland Ice Sheet (GrIS). The motivation is an increased mass loss (Sasgen et al., 2012; Shepherd et al., 2012; Svendsen et al., 2013) observed e.g. through a lowering of the ice surface mainly in margin regions, as found by Sørensen et al. (2011) using ICESat repeat-track data or by Khvorostovsky (2012), who used ERS-1, ERS-2 and Envisat cross-overs. In order to increase our understanding of the changes, four parameters are to be determined (ESA, 2013a):

- Surface Elevation Changes (SEC): 5 km × 5 km grids made from Envisat, ERS-1 and ERS-2 radar altimeter data. Once CryoSat-2 and Sentinel-3 data are available, they will be included in the analysis.

Discussion Paper | Discussion Paper | Discussion Paper | Discussion Paper |

– Ice Velocity (IV): 500 m × 500 m maps from repeat-pass SAR data over coastal outlet glaciers such as Jakobshavn Isbræ and Upernavik Isstrøm.

– Calving Front Locations (CFL): 250 m × 250 m shape-files of marine terminating glaciers or ice streams such as Jakobshavn Isbræ and Kangerdlugssuaq. Optical data from e.g. MERIS and MODIS will be used.

– Grounding Line Locations (GLL): 250 m × 250 m shape-files of marine terminating glaciers with a floating-tongue, e.g. the Petermann and 79-fjord glaciers. Optical, altimetric and InSAR data will be used.

The work is carried out through a broad collaboration between relevant cryospheric and climate-related research groups across Europe. The international aspect is further increased through the so-called Round Robin (RR) exercise performed in all the 13 projects. The goal of this exercise is to find the optimal method for estimating the given climate variable parameters; in order to understand exactly how this is best done members of the international scientific community were contacted and encouraged to submit their best estimate along with an in-depth description of the applied method. Here, we present the outcome of the RR exercise with a particular focus on SEC. The submitted results are inter-compared and validated against airborne laser scanner data, and the resulting conclusions form the basis of the final GrIS SEC production. As mentioned previously, this will be based on radar altimetry, and cf. e.g. Bamber et al. (2001) and Zwally et al. (2005) such data are highly applicable for surface change detection.

2 About the Round Robin exercise

For the Ice Sheets CCI, the RR was announced through personal invitations as well as postings on CRYOLIST and the CCI web-site (http://www.esa-icesheets-cci.org/). In order to establish a basis for inter-comparing the results, the participants were given an observation area as well as data to be used. They were then asked to submit their

best estimates of the given parameters along with errors and a feedback sheet describing computer specifications, pre- and post-processing steps as well as estimation specifications, computational time, man hours, etc. This allowed for a thorough inter-comparison of the various applied methods and thus for finding the optimal ones to be used for deriving the four parameters. The personal invitations gave the highest success-rate, and 26 researchers from Europe and the US responded providing SEC with 11 submissions, IV with 9, CFL with 6, and GLL with 0.

The results in focus here are those from SEC in which either ICESat laser or Envisat radar altimetry data could be used over the Jakobshavn Isbræ drainage basin (68–71° N; 39–52° W). In case the participants needed an external DEM to carry out the analysis, it was recommended to use the GIMP DEM developed by Howat et al. One of the 11 submissions was discarded as the results were either comparable with the remaining datasets or independent of the validation data.

Table 1 shows the sensor and method used by the participants as well as the submitted output parameters and whether the participants have applied a slope correction (Scharrer et al., 2013). In order to anonymise the RR results, the participants are referred to as SEC-1, SEC-2,. . . , SEC-10, the order in which they are named being random. Three participants used Envisat data and the remaining seven worked with ICESat. Of these, five groups applied the cross-over technique (XO), while the remaining five used repeat-tracks (RT) (Gunter et al., 2013; Slobbe et al., 2008; Moholdt et al., 2010). Slope corrections were only applied in two cases: SEC-1 used a Point of Closest Approach (POCA) method, while SEC-2 used plane fitting to correct for the slope.

Some groups submitted both elevation time series and SEC estimates. In the former, a formation of time series is first made, e.g. one for each grid cell, after which typically linear least-squares is used to fit a trend to the surface elevations. The direct estimates are made when fitting a trend to elevation differences (dH) vs. the temporal difference between the data acquisition times (dt).

The above differences in the datasets and their formation made it possible to perform an inter-comparison of the methods and approaches. The following parameters were therefore analysed:

- radar vs. laser altimetry,
- cross-overs vs. repeat-track.

A final part of the RR was to validate the results. This was done using airborne LiDAR data from ESA's CryoVex and NASA's IceBridge campaigns, due to the observations' high accuracy and spatial resolution.

2.1 Temporal extent and spatial resolution

Table 2 lists the spatial resolution and temporal extent of the submissions. The latter was found to mainly be based on the operational period of the sensor in question. Two Envisat datasets span the period from 2002–2010 corresponding to the 35 day repeat cycle, while the last dataset covers the ICESat observation period from 2003–2009. This is also the case for the ICESat datasets, which, however, are limited by the period of active laser altimeters. No Envisat datasets cover the period from the lowering of the satellite in October 2010 until it ceased operation in March 2012. This, however, makes the submissions more easily comparable, see Sect. 3.2.

The spatial resolution and density of prediction points depend on the applied method. Repeat-tracks have a higher spatial resolution than cross-overs due to the better ground coverage, and the vertical resolution is typically higher for laser rather than radar data as laser altimeters have a higher vertical accuracy and thus lower random errors; e.g. Brenner et al. (2007) found a laser precision of 0.14–0.59 m and a radar precision of 0.28–2.06 m, depending on the surface slope. The grid cells either along-track (RT) or throughout the observation area (XO) vary in size from hundreds of meters to several km. The along-track results are interpolated to the mean-repeat track position, and SEC-3's prediction points are constrained to the actual drainage basin.

3 Results

The following sections present the results submitted by the Round Robin participants along with their inter-comparison and validation. The latter is conducted using airborne LiDAR data.

3.1 The Round Robin exercise

Figures 1–2 show the participants' location of prediction points, the elevation change estimates (Fig. 1), and the corresponding errors (Fig. 2). The XO errors are calculated as the standard error of the trend, while the method for finding the remaining estimates is unknown. In spite of this, they do, however, provide important information on the accuracy of the different instruments and methods and thus are included after all. The results are presented according to the use of RT and XO, respectively.

The RT results are given in dense grids covering the entire observation area, and both radar and laser altimetry resolve the SEC values quite well. SEC-1's Envisat results (Fig. 1, top, left) are particularly interesting as they illustrate the possibility of using radar altimetry to observe surface changes even along the ice margin where surface topography, due to high slopes and undulations, as well as surface penetration of the radar pulses distort the signal (Brenner et al., 1983; Ridley and Partington, 1988).

The estimates from the two sensors agree well in the interior whereas a small offset is found by the ice margin where ICESat data (SEC-2–SEC-5) show a larger thinning. This is due to its ground tracks agreeing better with the glacier outlet as Envisat misses the smaller ice streams. In addition, differences between the two sensors arise from the ICESat observation period being shorter by two years, ICESat's smaller footprint size (70 m vs. 2–10 km), which allows for a more realistic change detection, as well as errors in the slope correction, the latter being an integral part of the Envisat data processing (Hurkmans et al., 2012).

The footprint size is particularly important in coastal regions as it determines the amount of topography being included in the signal; for Envisat this along with the slope

Discussion Paper | Discussion Paper | Discussion Paper | Discussion Paper |

correction error introduce the largest errors, and thus surface topography, penetration of the pulses, and varying footprint sizes explain why the largest errors generally are found in this area. Most errors reach approximately 3 $\mathrm{m\,yr^{-1}}$, while further inland they decrease to 0–1 $\mathrm{m\,yr^{-1}}$. The Envisat RT errors (Fig. 2 top, left) exceed those from ICESat (SEC-2 to SEC-5) by a few orders of magnitude. This is due to the reasons given above.

The cross-over points, SEC-6 to SEC-10 do not resolve the large thinning observed along the drainage basin and ice margin using RT. This can be explained by the inclination angles of ICESat (94°) and Envisat (98.6°) as well as the XO measurements being found by gridding the observations into cells, causing part of the signal to disappear as it is smoothed out during the process. As the RR participants have applied differently-sized grid cells, observations from the same sensor do not agree in space; the only overlap is found for SEC-7 and SEC-9, based on ICESat and Envisat, respectively, and possibly resulting from the submissions coming from the same research institution. The $\mathrm{d}H/\mathrm{d}t$ estimates in the interior parts of the ice sheet agree well for the two sensors as well as when compared with the RT results. This high accuracy of the results is confirmed when considering the error estimates (Fig. 2), which for most observations are on a sub-meter scale: 100 % of SEC-7 and SEC-9's errors are below 1 $\mathrm{m\,yr^{-1}}$, and the same is found for 99 % of SEC-8's results and 75 % of those from SEC-6. SEC-10 has not provided errors.

The results from the XO analyses have the highest accuracy as, e.g., slope effects can be ignored. However, because of the spatial density of ground tracks, XO points are limited in space. The opposite is observed with RT, which have a high spatial resolution however larger errors as the ground tracks are rarely exactly repeated thereby introducing interpolation errors into the results.

3.2 Inter-comparison of Round Robin results

In order to thoroughly analyse the methodologies supporting the submitted results, the following inter-comparisons are made (Fig. 3 and Table 3):

- *Radar: Repeat-track vs. cross-overs.* Both participants, SEC-1 and SEC-10, used Envisat data. SEC-1 applied the RT technique while SEC-10 used XO differences.
- *Laser: Repeat-track vs. cross-overs.* Both participants, SEC-3 and SEC-7, used ICESat data. SEC-3 applied the RT technique while SEC-7 used XO differences.
- *RT: Laser vs. radar altimetry.* Both participants, SEC-1 and SEC-3, applied the RT technique. SEC-1 used Envisat data and SEC-3 ICESat data.
- *XO: Laser vs. radar altimetry.* Both participants, SEC-8 and SEC-10, applied XO differences. SEC-8 used ICESat data and SEC-10 Envisat data.

The applied methodologies are assessed by finding overlapping prediction points and differencing the SEC values herein "*diff*"). The mean and root-mean-square-errors (RMSE) of these differences are then found while scatter plots reveal the R^2. The search radius for the overlaps is based on the spatial resolution of the observations (Table 2, column 4).

The analysis of the application of repeat-track vs. cross-overs shows the largest offsets among the submitted results, i.e. the highest RMSE and the lowest R^2. The RT values generally show a larger spread in $\mathrm{d}H/\mathrm{d}t$ than XO, and the radar data have a smaller R^2 (= 0.63) than the laser data (= 0.70). The different results are believed to arise from that mentioned in Sect. 3.1, namely the gridding of XO measurements into (differently-sized) cells thereby losing information on the SEC values as well as the opposing spatial resolution of the datasets: RT have a high density of measurements along-track, while XO measurements are restricted to overlapping ascending and descending ground tracks, both of which are sparse in time and space. This is also thought to explain the poor slopes of the results, which indicate that in spite of a relatively high R^2 the different methods to do not resolve the same signal.

The advantage of the RT method is exactly the high spatial resolution. However, as the ground tracks rarely coincide entirely, errors from slope effects are introduced when interpolating measurements from one track to the other. This is particularly relevant in a mountainous region such as by the ice margin, and thus also illustrates the advantage of XO measurements: the use of overlapping observations ensures that slope effects can be ignored thereby greatly reducing the uncertainty in this type of measurements.

The analyses of laser vs. radar data show that the RT and XO techniques give consistent results, and generally that radar data can be used to resolve Surface Elevation Changes even in regions with high topography equally well as laser altimetry. This is seen from the near-zero differences found between the $\mathrm{d}H/\mathrm{d}t$ estimates, the low RMSE, and the $R^2 = 0.90$ for both cases. All values show a good potential for the use of radar altimetry in the final SEC production, and thus that the issues with slope effects and different footprint sizes can be overcome. The RT analysis (SEC-3 vs. SEC-1) shows a larger spread in $\mathrm{d}H/\mathrm{d}t$ than the XO (SEC-8 vs. SEC-10), confirming that the RT data are able to better resolve the changes, large and small, than XO where the extreme SEC values are smoothed out due to averaging of the observations as well as their spatial distribution throughout the observation area.

3.3 Validation with airborne LiDAR data

The RR results presented in Fig. 1 are validated against SEC trends derived from airborne LiDAR data acquired with the laser scanners flown in ESA's CryoVex and NASA's IceBridge campaigns. In order to ensure a temporal consistency with the RR results two separate trends are derived, one from 2003–2009 and one from 2002–2010. The focus area is the main trunk of Jakobshavn Isbræ's outlet as this is where the largest surface changes are observed (Liu et al., 2012; Levinsen et al., 2013; Nielsen et al., 2013). As the largest errors are found in the same region, it is interesting to observe exactly how well the RR results do here. The LiDAR trends are derived using the model by Bamber et al. (2001) as a reference DEM and by fitting a trend as well as cyclic terms to a sequence of 500 m averaged LiDAR data. In order to ensure consistency with the RR data, the resulting validation trends have been estimated with a spatial resolution of 1 km, and for these to make a proper ground truth only data with a minimum of three observation periods are used.

Table 4 provides the results of the validation. As before, the difference between the LiDAR and RR $\mathrm{d}H/\mathrm{d}t$ trends ("$\mathrm{diff}_{\mathrm{lidar}}$") is found and the mean and standard deviations (std) are estimated. The RT results (SEC-1–SEC-5) show the largest offsets along the ice margin and north of the glacier basin; this can be attributed to slope effects. Other than that $\mathrm{diff}_{\mathrm{lidar}} \approx 0\,\mathrm{m\,yr^{-1}}$. The XO results from SEC-6 are consistent with the aforementioned both with respect to mean and std ($\mathrm{diff}_{\mathrm{lidar}}$), which are equally high. The remaining analyses (SEC-7–SEC-10) yield the best agreement between the LiDAR and RR trends. This is seen as the spread in std ($\mathrm{diff}_{\mathrm{lidar}}$) is significantly smaller than for any other method, and this is believed to result from the exploitation of cross-over points so slope effects can be disregarded. The SEC-9 mean value is relatively high, possibly because of the correspondingly high grid spacing (Table 2) and footprint size.

4 Discussion

Figure 4 outlines the results of the Round Robin exercise: generally agreeing $\mathrm{d}H/\mathrm{d}t$ values in the interior (high elevations) for all methods and disagreements further out along the ice margin (low elevations). The surface changes in the interior are small, and due to the little amount of topography both laser and radar altimetry perform well, regardless of the method. For the margin regions, the laser data typically indicate lower $\mathrm{d}H/\mathrm{d}t$ values, due to ICESat's ground tracks agreeing better with the actual outlet than those of Envisat. The XO results are all near-zero, which is due to the observation points being on high elevations, far from the glacier outlet, as well as averaging of the observations.

An interesting observation in the ICESat datasets is that although the participants have used the same data release (R33) and some the same method, e.g. RT (SEC-2–SEC-5), the results still differ. This is partly due to varying processing and estimation schemes, such as different data rejection criteria and linear least squares techniques, i.e. weighted, unweighted and multi-variate approaches, respectively. An additional reason is the inter-observation range biases, the so-called inter-campaign biases, which vary with time thereby affecting the accuracy of the ICESat elevation measurements. As different groups have obtained different bias estimates for the same dataset, a unique correction tool is necessary, and cf. Borsa et al. (2013) such one is currently underway (Hofton et al., 2012; Schutz et al., 2011).

Along with varying ways of determining the SEC errors (Fig. 2) as well as the lack of information submitted regarding exactly this, a difficulty arises in directly comparing the received datasets. In spite of this, the uniquity of the Round Robin exercise is the ability to evaluate the submissions regarding methodology, pre- and post-processing steps, computer specifications, the use of external datasets such as the GIMP DEM (Howat et al., 2012), etc. SEC-1's RT results illustrate the good potential of using radar altimetry to estimate SEC all the way to the ice margin, the inter-comparison with laser data confirms this, and thus it will be highly beneficial to include data from CryoSat-2 as well as Sentinel-3 once available.

The computation efforts, as indicated in the received feedback sheets, reveal that XO typically have the shortest processing times. This is seen in spite of e.g. SEC-4 (RT) and SEC-8 (XO) both applying unweighted linear least squares and one participant not using the tropospheric correction included in ESA's Envisat dataset. The external European Centre for Medium-Range Weather Forecasts (ECMWF) Re-Analysis ERA-Interim correction, derived from surface pressure, is implemented instead. However, the actual computation time depends on the implementation and optimization of the applied methods and hence is not a big issue for large-scale computations carried out on modern-day computers.

As mentioned in the Introduction, the final SEC grids will have a spatial resolution of 5 km × 5 km. This is found to be a sufficient trade-off between the resolution achievable with radar altimetry and the final accuracy of the results. Looking into the RR, the resolution is reasonable based on the promising radar RT results submitted by SEC-1, the sparsity of observation points when using XO, as well as the inter-comparisons (Fig. 3) e.g. showing that radar and laser data can perform equally well, everything considered. The reason for SEC-9 disagreeing so much with the LiDAR data is believed

to result from Envisat's larger footprint size as well as the spatial resolution, which, as is the case for SEC-7, greatly reduces the amount of estimation points. Based on the received results, a combination of RT and XO will allow for a high spatial coverage, and the 5 km × 5 km grid spacing is sufficient for accurately mapping SEC throughout the ice sheet, i.e. both in interior and margin regions.

Due to different observation periods and flight times, completely agreeing acquisition times of the data used in the RR analysis cannot be achieved. This will introduce a difference between the RR and LiDAR dH/dt trends, which, if not accounted for, affects the comparison of the two types of data. The LiDAR measurements are typically acquired in April/May or August, whereas ICESat data is only available in the periods of active lasers, i.e. approximately 35 days two to three times a year (NASA, 2013a, b). Thus, when comparing a trend based on LiDAR data obtained in May with one derived from altimetry data acquired in e.g. October/November, the intermediate Surface Elevation Changes must be accounted for.

This can be done using a Positive Degree Day model such as that by van den Broeke et al. (2010). It is based on the RACMO2/GR regional atmospheric climate model for Greenland (van Meijgaard et al., 2008) as well as observations from three Automatic Weather Stations located in Jakobshavn's ablation zone. It calculates the degree day factors for snow and ice, respectively, i.e. a measure of the melt per positive degree-day. Given knowledge on what is melting, an estimate of the vertical surface change can be found. Problems with such a model are e.g. the sparsity of weather stations throughout the ice sheet, the lack of observations of the exact composition of the surface material (e.g. ice, firn, or snow), the temporal change of the degree day factors due to changes in albedo, melt season length, etc. Further complications arise as it does not account for precipitation, for which the rates are highest in the southern parts of the GrIS. As the precipitation pattern changes in both time and space, the exact rates at which this happens is necessary in order to properly correct for the elevation change occurring due to different data acquisition times (Ettema et al., 2009; Sasgen et al., 2012).

The lack of observations also distort mass balance approaches where a flux-balance and seasonal mass balance estimates can be used to infer the vertical surface change. Additional error sources are the poorly known density needed for such estimates as well as the seasonal variability of all of the above.

This indicates the difficulty in estimating an accurate vertical correction term to be applied to the LiDAR SEC trends prior to using them for validating the RR datasets. However, when applying the model and using a threshold temperature of $T_0 = -5\,^{\circ}\mathrm{C}$ in order to include (nearly) all melt days it is found that the largest elevation difference from either snow or ice is a few meters, i.e. less than the dynamical thinning observed in the area.

5 Conclusions

In order to find the optimal method for determining Surface Elevation Changes (SEC) of the Greenland Ice Sheet, a so-called Round Robin exercise was performed as part of the ESA CCI Ice Sheets project. In this, researchers across Europe and the US submitted their best estimates for a pre-determined area, the Jakobshavn Isbræ drainage basin, derived using either radar (Envisat) or laser altimetry (ICESat) data. In order to evaluate the results, an inter-comparison of e.g. repeat-track (RT) vs. cross-overs (XO) and laser vs. radar data was performed. The submissions were validated against SEC trends derived from temporally consistent airborne LiDAR data from ESA's CryoVex and NASA's IceBridge campaigns. Through this the Round Robin conclusions can be summarised as follows:

- The spatial resolution of SEC estimates is higher with RT than with XO, and thus RT allows for better resolving the surface changes along the ice margin, such as along narrow ice streams.

- The SEC accuracy is higher with XO, at the cost of a lower spatial resolution. Thus, the application of XO is most suitable in the interior ice sheet.

- In spite of ICESat's smaller footprint size, the inter-comparison of laser and radar altimetry revealed that Envisat equally has the potential to map height changes even in regions with high topography. This shows good potential for a future implementation of ESA radar altimetry data from the up-coming Sentinel-3 mission; the first of three satellites is expected to be launched in 2014 (ESA, 2013b).

For the ESA CCI SEC generation, we therefore propose a hybrid method in which RT and XO results are combined in order to maximize the spatial resolution and minimize the estimation errors. This will be done using geostatistical interpolation tools, i.e. the optimal gridding procedures known from collocation/simple kriging (Dermanis, 1984; Goovaerts, 1997; Hofmann-Wellenhof and Moritz, 2005). The final output will be a gridded SEC product with a spatial resolution of 5 km × 5 km, and when to use which method – or both – is based on a weighting of the error variances. The grid will predominately consist of RT results near repeat ground tracks and along the ice margin, the latter due to their higher spatial resolution, while XO estimates are found where ascending and descending ground tracks intersect. Due to their high accuracy, these will be used over as large a region as possible.

The RT and XO algorithms are already implemented among the CCI project partners and the effort for merging them into a transparent and fully operational set-up is on-going. Thus, a prototype of Envisat SEC is currently available at the ESA web-site. The implementation of ERS data has begun, and once a full understanding of the accuracy and performance of CryoSat's InSAR altimeter has been reached, and the quality of the applied slope correction has been assessed, the inclusion of CryoSat-2 data will commence in order to bridge the gap between Envisat and Sentinel-3. The production of the final SEC grids is thereby underway.

Acknowledgements. We thank the Round Robin participants for their submitted datasets and elaborate feedback sheets. The study was supported by the European Space Agency (ESA) through the Ice_Sheets_CCI (4000104815/11/I-NB). Both the ICESat GLAS and ATM LiDAR data were downloaded from NSIDC while Envisat data were acquired through ESA. The CryoVex data were available in-house at DTU Space.

Author contributions: J. F. Levinsen performed the analysis and validation of the Round Robin submissions, wrote the paper and produced the figures. K. Khvorostovsky unified the submitted datasets and, along with F. Ticconi, A. Shepherd and R. Forsberg, assisted in data interpretation and in the discussion of how to develop the optimal SEC module. The remaining authors form the team of Round Robin participants and are listed in a random order, based on the affiliation. All co-authors contributed to the discussions leading to the results presented in the paper.

References

Bamber, J. L., Ekholm, S., and Krabill, W. B.: A new, high-resolution digital elevation model of Greenland fully validated with airborne laser altimeter data, J. Geophys. Res.-Sol. Ea., 106, 2001. 5437, 5443

Borsa, A. A., Moholdt, G., Fricker, H. A., and Brunt, K. M.: A range correction for ICESat and its potential impact on ice sheet mass balance studies, The Cryosphere Discuss., 7, 4287–4319, doi:10.5194/tcd-7-4287-2013, 2013. 5445

Brenner, A. C., Blndschadler, R. A., Thomas, R. H., and Zwally, H. J.: Slope-induced errors in radar altimetry over continental ice sheets, J. Geophys. Res.-Oceans, 88, 1617–1623, doi:10.1029/JC088iC03p01617, 1983. 5440

Brenner, A. C., DiMarzio, J. P., and Zwally, H. J.: Precision and accuracy of satellite radar and laser altimeter data over the continental ice sheets, IEEE T. Geosci. Remote, 45, 321–331, doi:10.1109/TGRS.2006.887172, 2007. 5439

Dermanis, A.: Kriging and collocation – a comparison, Manuscripta Geodaetics, 9, 159–167, 1984. 5448

ESA: ESA Climate Change Initiative, available at: http://www.esa-cci.org/, 2011. 5436

ESA: Ice Sheets Essential Climate Variable, available at: http://www.esa-icesheets-cci.org/, 2013a. 5436

ESA: Sentinel 3, available at: https://earth.esa.int/web/guest/missions/esa-future-missions/sentinel-3, 2013b. 5448

Ettema, J., van den Broeke, M. R., van Meijgaard, E., van de Berg, W. J., Bamber, J. L., Box, J. E., and Bales, R. C.: Higher surface mass balance of the Green-

land ice sheet revealed by high-resolution climate modeling, Geophys. Res. Lett., 36, doi:10.1029/2009GL038110, 2009. 5446

Goovaerts, P.: Geostatistics for Natural Resources Evaluation, Applied Geostatistics Series, Oxford University Press, Oxford, ISBN 0-19-511538-4, 1997. 5448

Gunter, B. C., Didova, O., Riva, R. E. M., Ligtenberg, S. R. M., Lenaerts, J. T. M., King, M. A., van den Broeke, M. R., and Urban, T.: Empirical estimation of present-day Antarctic glacial isostatic adjustment and ice mass change, The Cryosphere Discuss., 7, 3497–3541, doi:10.5194/tcd-7-3497-2013, 2013. 5438

Hofmann-Wellenhof, B. and Moritz, H.: Physical Geodesy, 2nd edn., Springer-Verlag, Wien, 2005. 5448

Hofton, M. A., Luthcke, S. B., and Blair, J. B.: Estimating ICESat-1 Inter-Campaign Elevation Biases at 86S Using LVIS Lidar Data, C21C-0632, American Geophysical Union – Fall Meeting, 2012. 5445

Howat, I. M., Negrete, A., Scambos, T., and Haran, T.: A high-resolution elevation model for the Greenland Ice Sheet from combined stereoscopic and photoclinometric data, available at: http://bprc.osu.edu/GDG/gimpdem.php, 2012. 5438, 5445

Hurkmans, R. T. W. L., Bamber, J. L., and Griggs, J. A.: Brief communication "Importance of slope-induced error correction in volume change estimates from radar altimetry", The Cryosphere, 6, 447–451, doi:10.5194/tc-6-447-2012, 2012. 5440

Khvorostovsky, K.: Merging and analysis of elevation time series over Greenland ice sheet from satellite radar altimetry, IEEE Trans. Geosc. Remote Sens., 50, 2012. 5436

Levinsen, J., Howat, I. M., and Tscherning, C. C.: Improving maps of ice-sheet surface elevation change using combined laser altimeter and stereoscopic elevation model data, J. Glaciol., 59, doi:10.3189/2013JoG12J114, 2013. 5443

Liu, L., Wahr, J., Howat, I. M., Khan, S. A., Joughin, I., and Furuya, M.: Constraining ice mass loss from Jakobshavn Isbræ (Greenland) using InSAR-measured crustal uplift, Geophys. J. Int., 188, 994–1006, doi:10.1111/j.1365-246X.2011.05317.x, 2012. 5443

Moholdt, G., Nuth, C., Hagen, J. O., and Kohler, J.: Recent elevation changes of Svalbard glaciers derived from ICESat laser altimetry, Remote Sens. Environ., 114, 2756–2767, doi:10.1016/j.rse.2010.06.008, 2010. 5438

NASA: Operation IceBridge – IceBridge Data Portal, available at: http://nsidc.org/icebridge/portal/, 2013a. 5446

NASA: Laser Operational Periods, available at: http://nsidc.org/data/icesat/laser_op_periods.html, 2013b. 5446
Nielsen, K., Khan, S. A., Spada, G., Wahr, J., Bevis, M., Liu, L., and van Dam, T.: Vertical and horizontal surface displacements near Jakobshavn Isbræ driven by melt-induced and dynamic ice loss, J. Geophys. Res.-Sol. Ea., 118, 1837–1844, doi:10.1002/jgrb.50145, 2013. 5443
Ridley, J. K. and Partington, K. C.: A model of satellite radar altimeter return from ice sheets, Int. J. Remote Sens., 9, 601–624, doi:10.1080/01431168808954881, 1988. 5440
Sasgen, I., van den Broeke, M., Bamber, J. L., Rignot, E., Sørensen, L. S., Wouters, B., Martinec, Z., Velicogna, I., and Simonsen, S. B.: Timing and origin of recent regional ice-mass loss in Greenland, Earth Planet. Sc. Lett., 333–334, 293–303, doi:10.1016/j.epsl.2012.03.033, 2012. 5436, 5446
Scharrer, K., Levinsen, J. F., and Ticconi, F.: Product Validation and Algorithm Selection Report for the Ice_Sheets_cci project of ESA's Climate Change Initiative, available from: http://www.esa-icesheets-cci.org/, 2013. 5438
Schutz, B., DiMarzio, J., Luthcke, S. B., Hancock, D., and Urban, T.: Notice Concerning Detection of ICESat/GLAS Inter-Campaign Elevation Biases, National Snow & Ice Data Center, August, 2011. 5445
Shepherd, A., Ivins, E. R., A, Geruo, Barletta, V. R., Bentley, M. J., Bettadpur, S., Briggs, K. H., Bromwich, D. H., Forsberg, R., Galin, N., Horwath, M., Jacobs, S., Joughin, I., King, M. A., Lenaerts, J. T. M., Li, J., Ligtenberg, S. R. M., Luckman, A., Luthcke, S. B., McMillan, M., Meister, R., Milne, G., Mouginot, J., Muir, A., Nicolas, J. P., Paden, J., Payne, A. J., Pritchard, H., Rignot, E., Rott, H., Sørensen, L. S., Scambos, T. A., Scheuchl, B., Schrama, E. J. O., Smith, B., Sundal, A. V., van Angelen, J. H., van de Berg, W. J., van den Broeke, M. R., Vaughan, D. G., Velicogna, I., Wahr, J., Whitehouse, P. L., Wingham, D. J., Yi, D., Young, D., and Zwally, H. J.: A Reconciled Estimate of Ice-Sheet Mass Balance, Science, 338, 1183–1189, doi:10.1126/science.1228102, 2012. 5436
Slobbe, D., Lindenbergh, R., and Ditmar, P.: Estimation of volume change rates of Greenland's ice sheet from ICESat data using overlapping footprints, Remote Sens. Environ., 112, 4204–4213, doi:10.1016/j.rse.2008.07.004, 2008. 5438
Sørensen, L. S., Simonsen, S. B., Nielsen, K., Lucas-Picher, P., Spada, G., Adalgeirsdottir, G., Forsberg, R., and Hvidberg, C. S.: Mass balance of the Greenland ice sheet (2003–2008)

from ICESat data – the impact of interpolation, sampling and firn density, The Cryosphere, 5, 173–186, doi:10.5194/tc-5-173-2011, 2011. 5436
Svendsen, P. L., Andersen, O. B., and Nielsen, A. A.: Acceleration of the Greenland ice sheet mass loss as observed by GRACE: confidence and sensitivity, Earth Planet. Sc. Lett., 364, 24–29, doi:10.1016/j.epsl.2012.12.010, 2013. 5436
van den Broeke, M., Bus, C., Ettema, J., and Smeets, P.: Temperature thresholds for degree-day modelling of Greenland ice sheet melt rates, Geophys. Res. Lett., 37, doi:10.1029/2010GL044123, 2010. 5446
van Meijgaard, E., van Ulft, L. H., van de Berg, W. J., Bosveld, F. C., van den Hurk, B. J. J. M., Lenderink, G., and Siebesma, A. P.: The KNMI regional atmospheric climate model, version 2.1, Tech. Rep. KNMI Tech. Rep. 302, R. Neth. Meteorol. Inst., De Bilt, the Netherlands, available at: http://a.knmi2.nl/bibliotheek/knmipubTR/TR302.pdf, 2008. 5446
Zwally, H. J., Giovinetto, M. B., Li, J., Cornejo, H. G., Beckley, M. A., Brenner, A. C., Saba, J. L., and Yi, D.: Mass changes of the Greenland and Antarctic ice sheets and shelves and contributions to sea-level rise: 1992–2002, J. Glaciol., 51, 509–527, doi:10.3189/172756505781829007, 2005. 5437

Table 1. Sensors and methods used for the SEC production as well as the final data parameters submitted by the Round Robin participants.

Participant	Sensor	Method	Output parameters	Slope correction
SEC-1	Envisat	Repeat-track	$\mathrm{d}H/\mathrm{d}t$ (time series)	GIMP DEM: Relocation at POCA
SEC-2	ICESat	Repeat-track	$\mathrm{d}H/\mathrm{d}t$	Plane fitting
SEC-3	ICESat	Repeat-track	$\mathrm{d}H/\mathrm{d}t$	N/A
SEC-4	ICESat	Repeat-track	$\mathrm{d}H/\mathrm{d}t$	N/A
SEC-5	ICESat	Repeat-track	$\mathrm{d}H/\mathrm{d}t$	N/A
SEC-6	ICESat	Cross-overs	$\mathrm{d}H/\mathrm{d}t$	N/A
SEC-7	ICESat	Cross-overs	$\mathrm{d}H/\mathrm{d}t$, XO differences	N/A
SEC-8	ICESat	Cross-overs	$\mathrm{d}H/\mathrm{d}t$	N/A
SEC-9	Envisat	Cross-overs	$\mathrm{d}H/\mathrm{d}t$ (time series)	N/A
SEC-10	Envisat	Cross-overs	$\mathrm{d}H/\mathrm{d}t$ (time series)	N/A

Table 2. Observation period, spatial density and spatial resolution of the Round Robin SEC products.

Participant	Observation period	Spatial density	Spatial resolution
SEC-1	Sep 2002–Oct 2010	Along Envisat tracks	5.0 km × 5.0 km along-track segments
SEC-2	Oct 2003–Oct 2009	Along ICESat tracks	0.7 km × 0.5 km along-track segments
SEC-3	Feb 2003–Oct 2009	Along ICESat tracks	1.0 km × 1.0 km along-track segments
SEC-4	Oct 2003–Oct 2009	Along ICESat tracks	0.5 km × 0.5 km along-track segments
SEC-5	Sep 2003–Oct 2009	Along ICESat tracks	1.0 km × 1.0 km along-track segments
SEC-6	Feb 2003–Oct 2009	Grid cells covering 100 % of area	8.0 km × 8.0 km grid cells
SEC-7	Oct 2003–Oct 2009	Grid cells covering ~ 93 % of area	0.5° lat × 1° lon grid cells
SEC-8	Feb 2003–Oct 2009	Grid cells covering ~ 95 % of area	1.2 km × 1.2 km grid cells
SEC-9	Sep 2003–Oct 2009	Grid cells covering ~ 97 % of area	0.5° lat × 1° lon grid cells
SEC-10	Oct 2003–Oct 2010	Grid cells covering ~ 90 % of area	10.0 km × 10.0 km grid cells

Discussion Paper | Discussion Paper | Discussion Paper | Discussion Paper |

Table 3. Results from the inter-comparison of a selection of the Round Robin results. The search radius used for finding overlapping grid cells is based on the spatial resolution given in Table 2, while "diff" holds the difference between the dH/dt estimates obtained by the different groups in question.

Participants	Method	Sensor	Search radius [km]	mean (diff) [m yr^{-1}]	RMSE [m yr^{-1}]	R^2	Slope
SEC-1–SEC-10	RT vs. XO	Radar	10	−0.06	0.38	0.63	0.40
SEC-3–SEC-7	RT vs. XO	Laser	5	−0.25	0.96	0.70	0.01
SEC-8–SEC-10	XO	Laser vs. radar	10	0.07	0.26	0.90	1.04
SEC-3–SEC-1	RT	Laser vs. radar	5	0.08	0.24	0.90	1.04

Table 4. Results from the validation of the Round Robin results using LiDAR dH/dt trends. The search radius used for finding overlapping grid cells is 500 m while the temporal coverage corresponds to that of the RR submissions, i.e. either 2003–2009 or 2002–2010, respectively. "$\text{diff}_{\text{lidar}}$" gives the d$H$/d$t$ difference between the LiDAR and the Round Robin values.

Participant	mean ($\text{diff}_{\text{lidar}}$) [m yr^{-1}]	std ($\text{diff}_{\text{lidar}}$) [m yr^{-1}]
SEC-1	−0.35	3.16
SEC-2	0.33	2.57
SEC-3	0.09	1.40
SEC-4	0.48	3.36
SEC-5	0.31	5.49
SEC-6	0.74	3.62
SEC-7	1.43	1.67
SEC-8	−0.02	1.56
SEC-9	1.11	1.52
SEC-10	0.23	1.31

Discussion Paper | Discussion Paper | Discussion Paper | Discussion Paper |

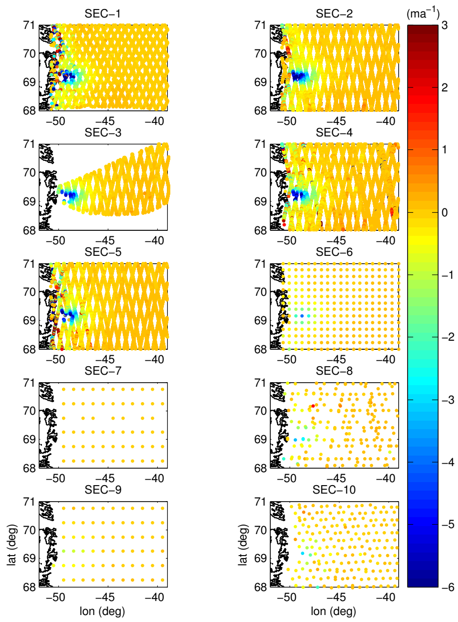

Fig. 1. Surface Elevation Changes derived using repeat-tracks (participants SEC-1 to SEC-5) and cross-overs (SEC-6 to SEC-10).

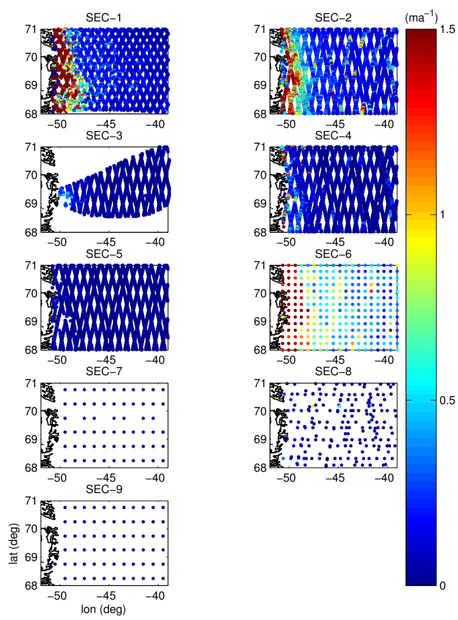

Fig. 2. Surface Elevation Change errors. Please notice that SEC-10 did not submit errors. The method for deriving the RT errors has not been described by the RR participants, whereas the XO errors are given as the standard error of the SEC trend.

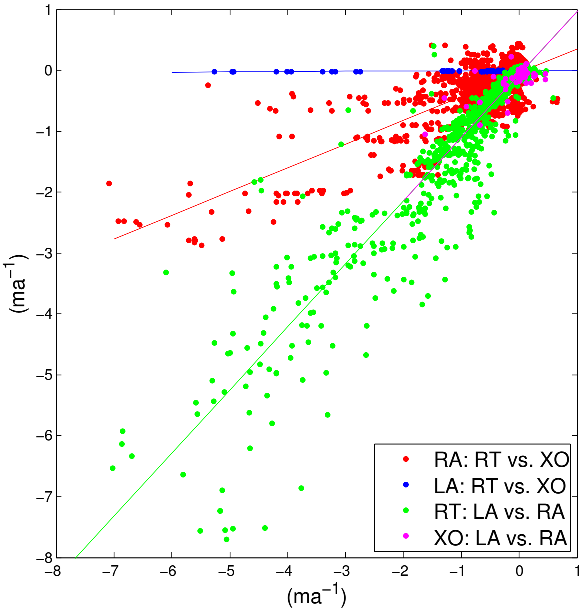

Fig. 3. Scatter plots from an inter-comparison of a selection of the Round Robin results: cross-overs vs. repeat-track for radar and laser altimetry (i.e. XO vs. RT for RA and LA, respectively) and radar vs. laser altimetry for both methods. See Table 3 for the RMSE and R^2 values.

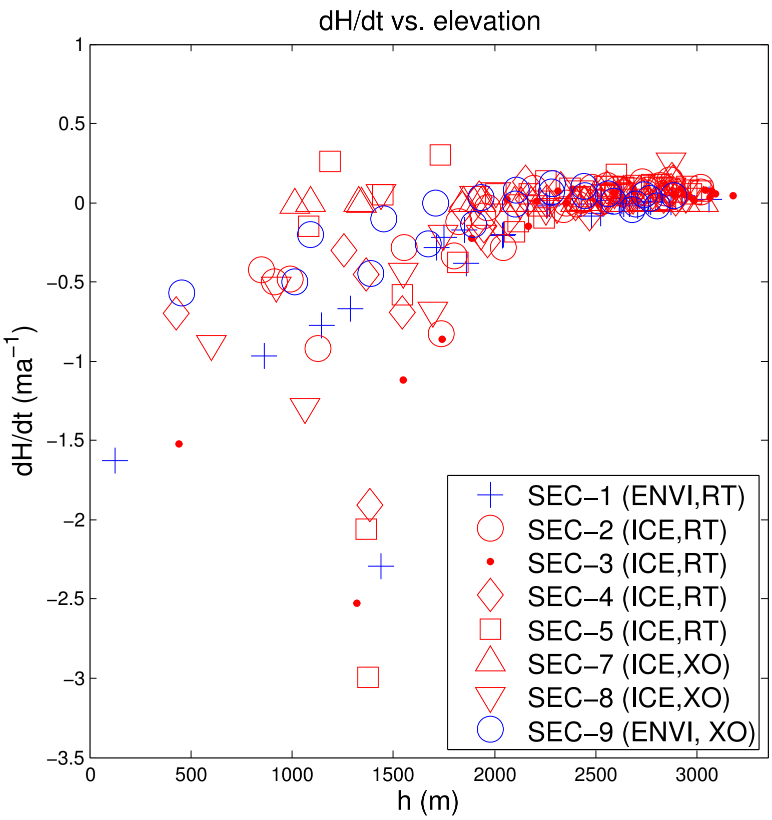

Fig. 4. Surface elevation vs. dH/dt. Notice that only a number of the participants have submitted elevations.

Discussion Paper | Discussion Paper | Discussion Paper | Discussion Paper |